

N O T I C E

THIS DOCUMENT HAS BEEN REPRODUCED FROM
MICROFICHE. ALTHOUGH IT IS RECOGNIZED THAT
CERTAIN PORTIONS ARE ILLEGIBLE, IT IS BEING RELEASED
IN THE INTEREST OF MAKING AVAILABLE AS MUCH
INFORMATION AS POSSIBLE

DOE/NASA/51044-15
NASA TM-81664

(NASA-TM-81664) CHARACTERIZATION OF THE
NEAR-TERM ELECTRIC VEHICLE (ETV-1)
BREADBOARD PROPULSION SYSTEM OVER THE SAE
J227a DRIVING SCHEDULE D (NASA) 15 p
HC A02/MF A01

N81-15465

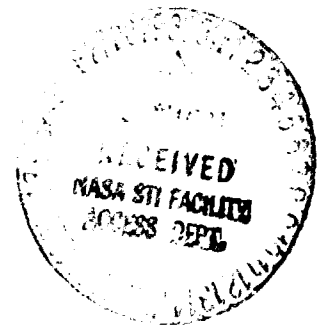
Unclas
29701

CSSL 10B G3/44

Characterization of the Near-Term Electric Vehicle (ETV-1) Breadboard Propulsion System Over the SAE J227a Driving Schedule "D"

Noel B. Sargent and Miles O. Dustin
National Aeronautics and Space Administration
Lewis Research Center

Work performed for
U.S. DEPARTMENT OF ENERGY
Conservation and Solar Energy
Office of Transportation Programs



Prepared for
Society of Automotive Engineers
International Congress and Exposition
Detroit, Michigan, February 23-27, 1981

Characterization of the Near-Term Electric Vehicle (ETV-1) Breadboard Propulsion System Over the SAE J227a Driving Schedule "D"

Noel B. Sargent and Miles O. Dustin
National Aeronautics and Space Administration
Lewis Research Center
Cleveland, Ohio 44135

Work performed for
U.S. DEPARTMENT OF ENERGY
Conservation and Solar Energy
Office of Transportation Programs
Washington, D.C. 20545
Under Interagency Agreement DE-AI01-77CS51044

Prepared for
Society of Automotive Engineers
International Congress and Exposition
Detroit, Michigan, February 23-27, 1981

CHARACTERIZATION OF THE NEAR TERM ELECTRIC VEHICLE (ETV-1) BREADBOARD
PROPULSION SYSTEM OVER THE SAE J227a DRIVING SCHEDULE "D"

Noel B. Sargent
Miles O. Dustin

National Aeronautics & Space Administration
Lewis Research Center
Cleveland, Ohio, U.S.A

ABSTRACT

The NASA-LeRC under the direction of DOE is responsible for the test and evaluation of electric and hybrid vehicle propulsion systems and components. In September 1978, a contracted effort was undertaken with the General Electric Company to design, fabricate, and deliver a propulsion system breadboard of the GE-NTEV (ETV-1). This breadboard is currently under test in the LeRC Road Load Simulator and its operational characteristics are the subject of this paper.

THE ELECTRIC TEST VEHICLE-ONE (ETV-1) was built by General Electric Company and Chrysler Corporation for the U.S. Department of Energy (DOE) to represent an electric vehicle designed and built from the ground up with present state-of-the-art technology. Two vehicles were built and are presently being evaluated by NASA's Jet Propulsion Laboratory (JPL). Some results of these JPL tests are also being presented at this conference. A duplicate set of propulsion system components were built, mounted on a breadboard, and delivered to NASA's Lewis Research Center for testing on the newly acquired Road Load Simulator (RLS). Lewis Research Center is responsible for the development, test, and evaluation of electric and hybrid vehicle propulsion systems and components for the Department of Energy. The breadboard is currently under test. This paper will describe driving cycle tests that have been completed on the system.

ETV-1 PROPULSION SYSTEM

The ETV-1 propulsion system is a good example of what can be done to maximize system efficiency using a state-of-the-art dc shunt motor, transistor armature and field choppers, and a

constant ratio speed reduction and differential unit.(1)* A complete set of these components were assembled on a breadboard for test on the Lewis Road Load Simulator. The major difference between the breadboard system and the systems used in the ETV-1 vehicle was that a torque transducer was installed between the motor and the speed reduction unit to measure motor output torque. Other minor differences included the wiring harness and small differences in component mounting and orientation necessitated by the breadboard concept. The fully instrumented propulsion system is shown in Figure 1. A schematic representation of the breadboard is shown in Figure 2. Component specifications are listed in Table 1.

The propulsion system operates in two separate modes depending on vehicle speed. Below base speed, which occurs at 25 mph, the motor is controlled by a chopper in the armature circuit. Above 25 mph the armature chopper is bypassed and the armature receives full battery voltage. Motor torque is then controlled by the field chopper.

The constant ratio speed reduction and differential unit consists of a double reduction "Hi-Vo" chain driving a geared automotive differential.

ROAD LOAD SIMULATOR TESTS

TEST FACILITY-The Road Load Simulator provides a means for applying the road torque to a propulsion system that the system would normally experience in a vehicle.(3) These torques are made up of a combination of tire losses, aerodynamic drag, road grade, and vehicle inertial loads. These combined torques can be represented by the torque equation:

$$T_{net} = K_1 + K_2V + K_3V^2 + K_4 \frac{d}{dt}V + K_5 \sin \theta \quad (1)$$

Where V_1 is vehicle speed and coefficients K_1 through K_5 relate to the tire friction, frontal area, aerodynamic drag, inertial torque and road grade angle, θ respectively. The torque loads that result from tire losses, aerodynamic losses and road grade are generated by a hydroviscous absorber. The inertial load is provided by flywheels. A schematic of the Road Load Simulator is shown in Figure 3.

*Numbers in parentheses designate references at end of paper.

Dustin

Speed Control-Speed control of the propulsion system is provided by a special automatic control system which is part of the RLS facility. This system takes the place of the vehicle driver in maintaining the correct vehicle speed over the driving cycle (SAE J227a, "D" schedule). A schematic of the speed control system is shown in Figure 4. The ETV-1 propulsion system control requires enabling signals to be present before either the acceleration or deceleration commands can be applied to the system. These enabling signals must be supplied by the RLS facility speed control system. The enabling signals are generated by differentiating the speed command signal. If the slope of the speed command signal is positive, the acceleration enable is actuated. If the slope is negative, the deceleration enable is actuated. A separate acceleration signal is generated by a three-function speed controller. If this signal is positive the ETV-1 propulsion system controller receives an acceleration command. If the RLS facility speed controller output is negative, the signal is split just as it is in the ETV-1 vehicle where 70% of the braking effort is applied to regenerative braking and the remaining 30% of the braking effort is applied to the vehicles' mechanical brakes. In this case, 70% of the braking effort is applied to the regenerative braking control (decel command) within the ETV-1 control and 30% is fed back to the RLS torque control as shown in Figure 4 to simulate vehicle mechanical brakes. The speed command signal is developed by an arbitrary waveform function generator. The desired speed-time profile is programmed into the waveform function generator, which produces the desired profile in a repetitive manner needed to conduct range tests on the propulsion system.

Instrumentation-A schematic representation of the propulsion system indicating major measurement locations is shown in Figure 5. These measurements separate the individual component performance and power flow through the system. Power is measured at the mechanical shafts by inline torque meters with integral speed transducers. Electrical power is measured with the appropriate current-voltage pairs with wide-band wattmeters.(4) The estimated accuracy for determining the efficiency of each component is ±2 percent. The power measurements in addition to average voltage, current and temperature data are recorded and processed on the Lewis Research Center central data system.

TEST PROCEDURE

Tests on the ETV-1 propulsion system measured detailed component efficiencies and system performance characteristics free of vehicle and track related variances. The tests reported here determined these characteristics over the SAE J227a Driving Schedule "D".

Procedure-Before meaningful tests can be performed on a propulsion system it is necessary to establish the correct coefficients for the road load equation.

$$F = W (f_1 + f_2 V) + .00241 C_D A V^2 \quad (2)$$

Where: F = Road Load, lb

W = Vehicle Weight, lb

f₁ = Time Coefficient, lb/lb of Vehicle Weight

f₂ = Time Coefficient, lb/lb of Vehicle Weight/mph

V = Vehicle Velocity, mph

C_D = Aerodynamic Drag Coefficient

A = Vehicle Frontal Area, ft²

Carefully controlled coastdown tests were conducted on the ETV-1 vehicle by JPL on a concrete runway at the Edwards Air Force Base. The runway grade is 0.177% and the wind velocity was less than 2 mph. The half axles and disc brakes were removed to assure that only the tires and wheel bearings affected the road load.

In order to duplicate vehicle characteristics with the RLS, identical coastdown tests were conducted on the RLS. The K₁, K₂, and K₃ factors were changed until a good match with the JPL coast down results was obtained. The JPL coastdown test is compared with the RLS coastdown test in Figure 6. The calculated road load coefficients using this technique are:

$$f_1 = .0095 \text{ #/#}$$

$$f_2 = 0$$

$$CdA = 6.4 \text{ ft}^2$$

The vehicle weight was 3900 pounds.

TEST RESULTS

The test program that will be conducted on the GE-ETV-1 propulsion system will include both steady state and driving cycle tests. Only driving cycle tests will be reported in this paper. The tests were conducted over driving schedule "D" of the SAE J227a Electric Vehicle Test Procedure. A typical velocity profile is shown in Figure 7. The dashed curve is the specified speed profile of the J227a. An actual speed profile from the ETV-1 breadboard propulsion system tests is shown by the solid curve. The acceleration speed-time profile is programmed on the RLS arbitrary Waveform Function Generator to extract energy from the battery at constant power.

Typical motor and transaxle torques required to propel the vehicle over the "D" cycle are shown in Figure 8. The torque scale for the speed reducer has been multiplied by the overall speed reduction ratio of 5.48 so that, except for speed reducer losses, the curves would coincide.

Battery power output over a typical cycle is shown in Figure 9. The curve shows a near constant power during the acceleration phase. It is interesting to note that battery power is greater during the 10 second long coast period

(78-88 seconds) than during the 9 second braking period (88-97 seconds). The theoretical kinetic energy removed from the vehicle during the coast period is defined by the equation:

$$KE = \frac{1}{2} \frac{W}{g} (V_1^2 - V_2^2) \quad (3)$$

Where: K.E = Kinetic Energy

W = Vehicle Weight

g = Gravitational Constant

V₁ = Velocity At End Of Cruise

V₂ = Velocity At End Of Coast

During the coast period 58 watt-hours of energy are removed from the vehicle, while during the brake period only 41 watt-hours are removed. In terms of theoretical average mechanical power, 20.9 kW is required to slow the vehicle from 45 mph to 29 mph (coast) and only 16.5 kW average power is required to slow the vehicle from 29 mph to 0 mph (braking). This analysis does not consider the road load losses during these periods.

To better illustrate where the major losses in the system occur, the losses for the three major components are plotted as a function of time over the driving cycle in Figure 10. As expected the major losses occur in the motor. The speed reduction unit losses are fairly constant. Motor, controller, and speed reducer efficiencies over typical "D" cycles are shown in Figures 11, 12, and 13.

Temperature Effects-During the driving cycle tests temperatures of the components were measured and recorded. The average motor temperature was determined by averaging the measurements of thermocouples buried in each of the four field windings. Two thermocouples located in the lubricating oil sump were averaged for the speed reducer temperature. The battery temperature was determined by averaging the readings of thermocouples placed in one cell of each of the battery modules. The variation in the average temperatures of these components over an entire range test are shown in Figure 14.

Previous steady state 45 mph constant speed tests conducted on the RLS determined that motor efficiency increased by about 3% as the motor temperature went from 80°F to 140°F. The efficiency is also influenced by the change in the state-of-charge of the battery. The magnitude of the state-of-charge effects have not yet been determined. The speed reducer efficiency increased by about 1% over the same temperature change. During the driving cycle tests, component efficiencies were determined during the cruise portion of each cycle. The change in component efficiency as the test was run is shown in Figure 15. The efficiency changes most rapidly during the early cycles since it is during this portion of the test that the fastest temperature rise is experienced.

Energy Economy-Table II lists the energy removed from the battery terminals and the energy output at the axle shaft during the combined acceleration and cruise portions and during the combined coast and brake portions of a typical cycle. Also listed in the table are the system efficiencies calculated for both the motoring portions of the cycle (acceleration and cruise) and for the regeneration portions (coast and brake).

Energy economy defined by SAE J227a involves measuring the total energy that is returned to the battery by the charger following a range test. During the RLS evaluation of the ETV-1, the on-board charger was not working properly and was not used. Therefore, energy economy as defined by SAE J227a cannot be used for the evaluation. The average economy based on battery output energy was 231 Wh/mi.

Range-The tests were conducted with the EV2-13 batteries (see Table I) delivered with the propulsion system. Due to delays in conducting the tests, the batteries had been stored for a long period and no longer had the specified capacity of 174 amp hours (at the 3 hour rate or 58 amps). Therefore tests to determine the range of the vehicle on the EV-2-13 batteries were not conducted.

CONCLUDING REMARKS

The performance of the GE/Chrysler ETV-1 propulsion system was evaluated in the Lewis Road Load Simulator. The ETV-1 propulsion system represents a well designed, well integrated system optimized for the "D" schedule driving cycle. The use of an armature chopper for operation below base speed results in high system efficiency over most of the "D" cycle.

Care must be exercised in applying the results of any dynamometer test. Although the problems of variable wind, temperature and test track grade are avoided in dynamometer tests other factors must be considered especially when evaluating short range vehicles such as electrics. Independent tire tests (5,6,7) have shown that tire resistance can drop considerably during the first hour of operation depending upon vehicle speed, tire inflation pressure, type of tire, etc. One example of temperature effects determined by Goodyear Tire and Rubber Company (5), shows the rolling resistance dropping from about 21 pounds per 1000 pounds of vehicle weight to 14 pounds as the tire ran for 50 minutes. Tests at Firestone Tire and Rubber Company (7) indicate that the rolling resistance of a typical tire can decrease by 50% as the ambient temperature goes from 40°F to 100°F. Since at 45 mph the rolling resistance of the tires represents about 50% of the total vehicle road load, a 50% change in the tire rolling resistance (for example, from 20 to 10 pounds per 1000 pounds of vehicle weight) would cause a 25% drop in total road load. The real range of the vehicle as a result will be considerably less than a range test conducted with previously warmed tires would indicate.

To determine more precisely the effect of tire temperature on the range of electric vehicles, fully instrumented tire tests should be run over a range of temperatures for various constant speed and driving cycle conditions. The results could then be used to develop better testing techniques for dynamometer system evaluations as well as better representation of real conditions for computer simulations.

REFERENCES

1. J.W.A. Wilson, "The Drive System of the DOE Near-Term Electric Vehicle (ETV-1)," SAE Paper No. 800058, February 1980.
2. "Near Term Electric Vehicle - Phase II - Final Report," SRD-79-076, General Electric Co., Schenectady, NY, March 1980.
3. N. B. Sargent, "A Laboratory Facility for Electric Vehicle Propulsion System Testing" DOE/NASA/11011-32, NASA TM-81574, September 1980.
4. D. Lesco, "Specifying and Calibrating Instrumentation for Wideband Electric Power Measurements," NASA TM-81545, 1980.
5. W. W. Curtiss, "Low Power Loss Tires" SAE Paper No. 690108, January 1969.
6. D. J. Schuring, "Transient Versus Steady-State Tire Rolling Loss Testing," SAE Paper No. 790116, March 1979.
7. H. L. Janssen, and G. L. Hall, "Effect of Ambient Temperature on Radial Tire Rolling Resistance," SAE Paper No. 80090, February 1980.

Table I-ETV-1 Component Specifications

Motor

Type - dc shunt, force ventilated
 Power Rating - 15 kW, continuous
 Voltage - 108V
 Maximum Speed - 5,000 rpm

Controller

Type - Transistorized, armature chopper, field chopper, microprocessor controlled
 Maximum Current - 400 amps motoring, 200 amps regenerative braking
 Cooling - Forced air

Speed Reducer and Differential

Type - 2-stage chain reduction
 Ratio - 5.48
 Differential - Omni/Horizon, modified

Batteries

Type - Globe-Union EV-2-13, lead-acid
 Voltage - 108 volts (18 - 6V modules)
 Weight - 1,092 pounds
 Capacity - 174 amp-hours (3hr. rate)

Table II-Summary of Energy Data

E_B , out (acceleration & cruise) = 280 W-hr.

E_B , in (coast & brake) = 54 W-hr.

E_T , out (acceleration & cruise) = 212 W-hr.

E_T , in (coast & brake) = 71 W-hr.

$$\eta_{s, out} = \frac{E_T, out}{E_B, out} = 75.7\% \text{ (motoring)}$$

$$\eta_{s, in} = \frac{E_B, in}{E_T, in} = 76.1\% \text{ (regenerative braking)}$$

$$\% \text{ Energy Returned to Battery} = \frac{E_B, in}{E_B, out} = 19.3\%$$

where:

E_B - Energy at Battery Terminals

E_T - Energy at Axle Shaft

η_s - System Efficiency

Note: The values used in this table were taken midway into the test (20th cycle).

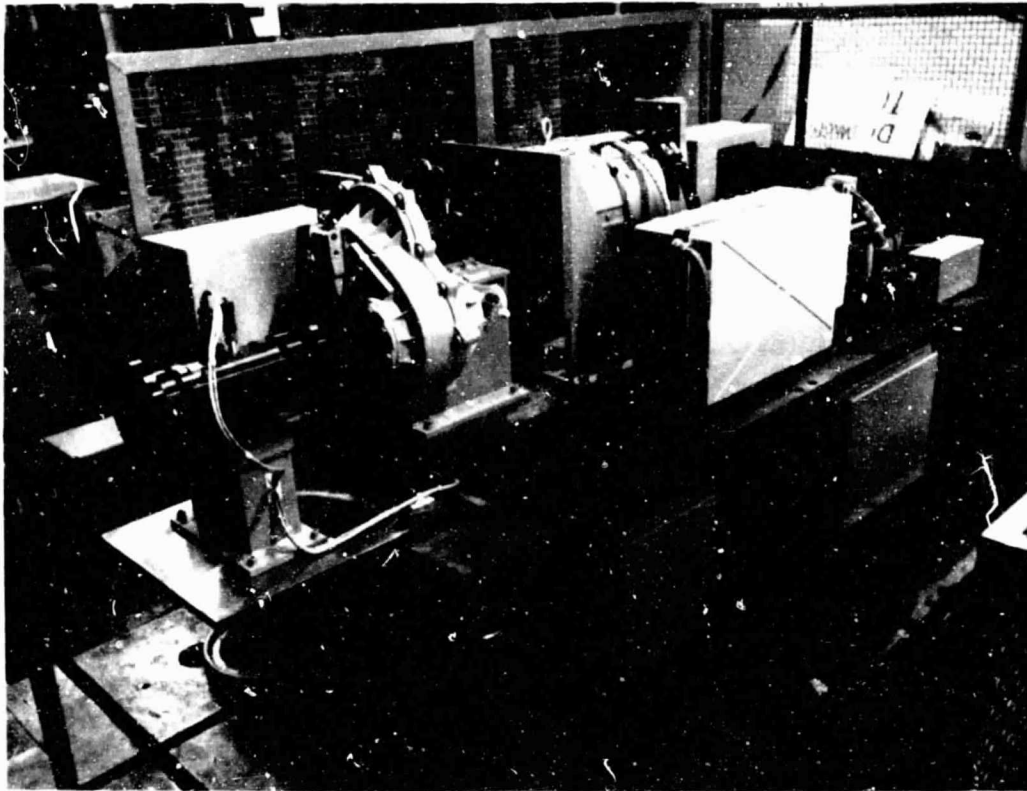


Figure 1. - ETV-1 propulsion system breadboard.

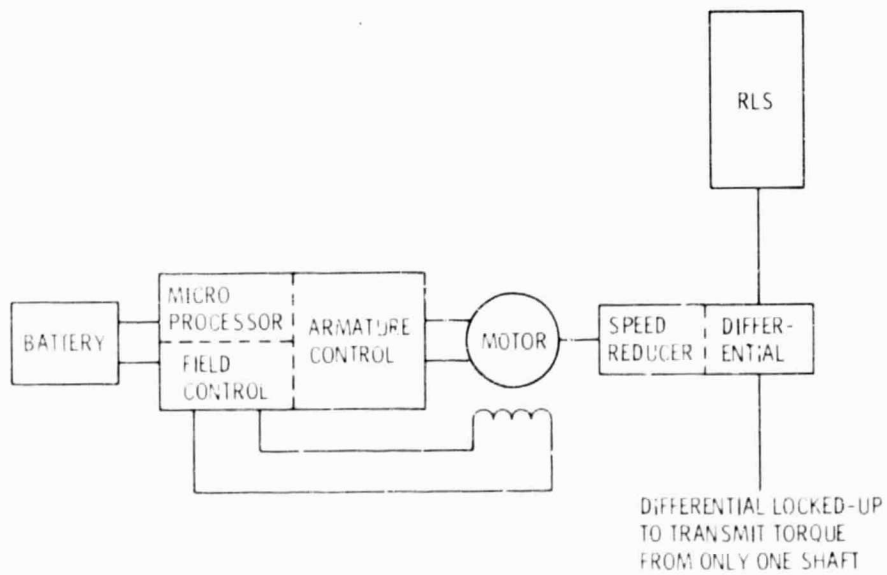


Figure 2. - ETV-1 propulsion system.

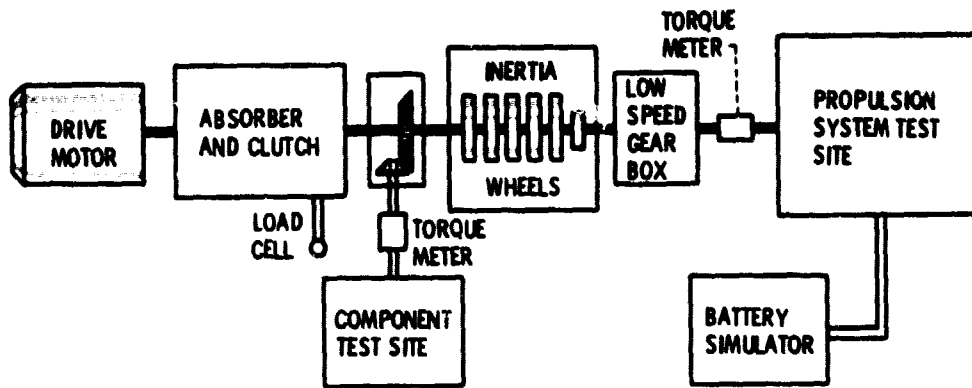


Figure 3 - Road load simulator schematic.

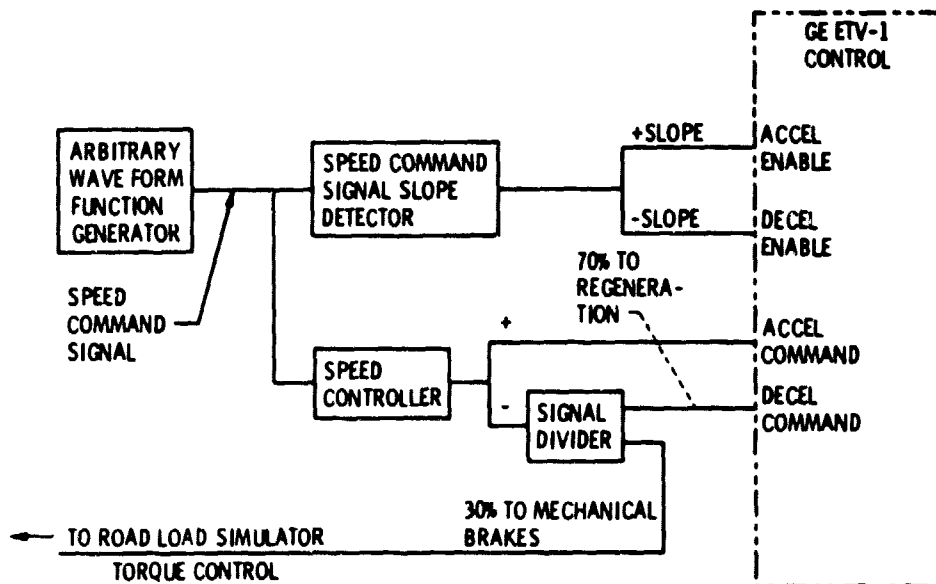


Figure 4 - Schematic of speed control system.

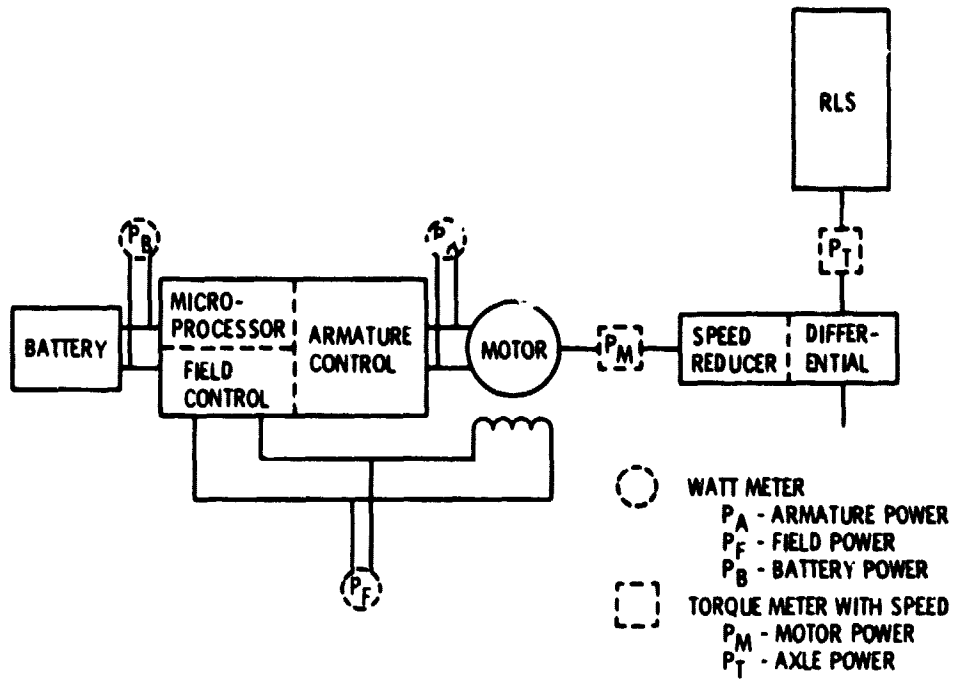


Figure 5. - Instrumentation to test ETV-1 propulsion system.

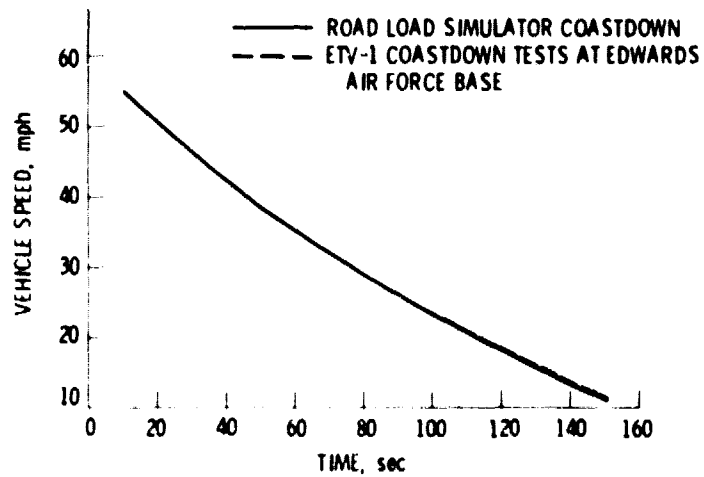


Figure 6

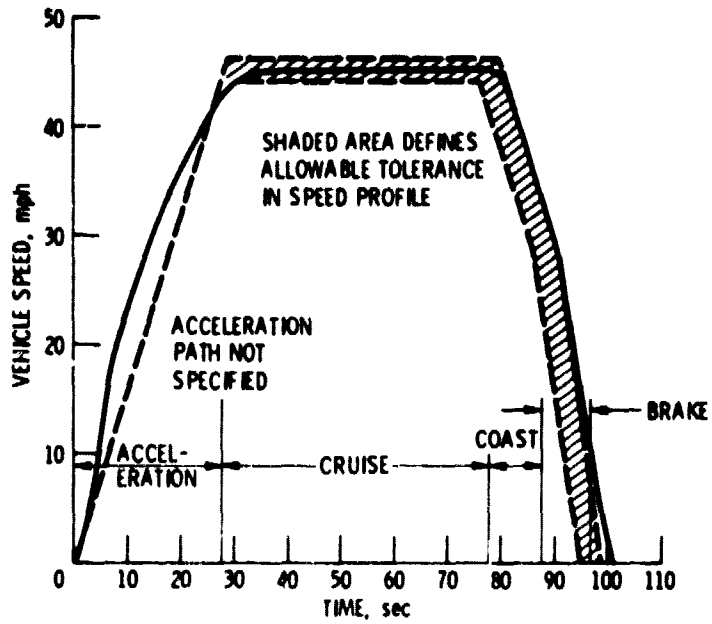


Figure 7. - Speed as a function of time for SAE J227a schedule "D" driving cycle.

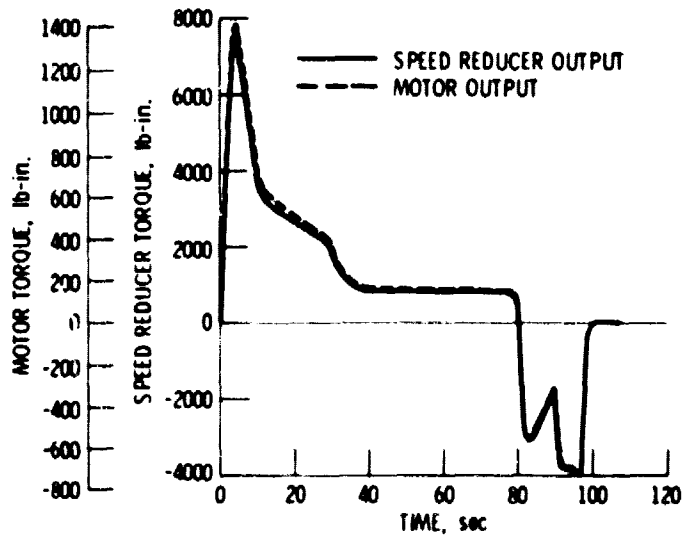


Figure 8. - Motor and speed reducer torque during SAE J227a driving schedule "D".

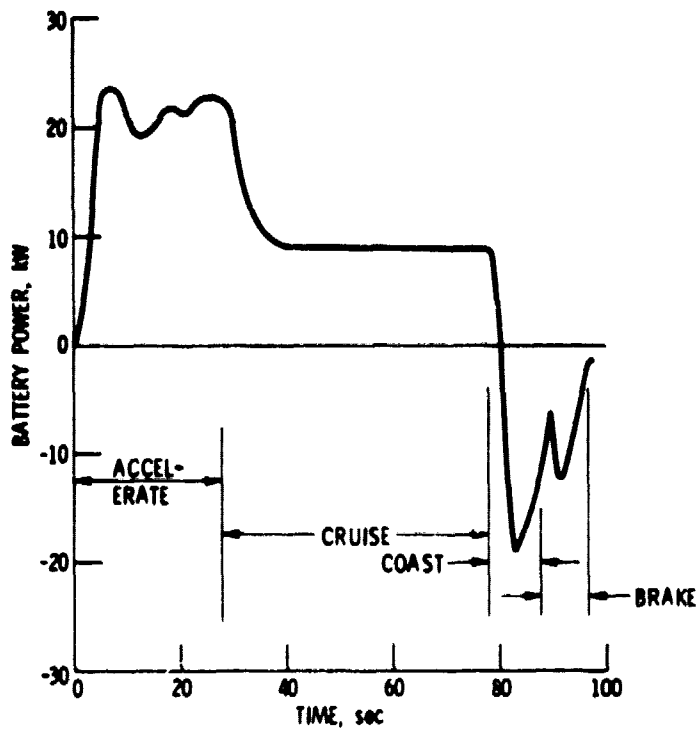


Figure 9. - Battery power as a function of time for SAE J227a schedule "D" driving cycle.

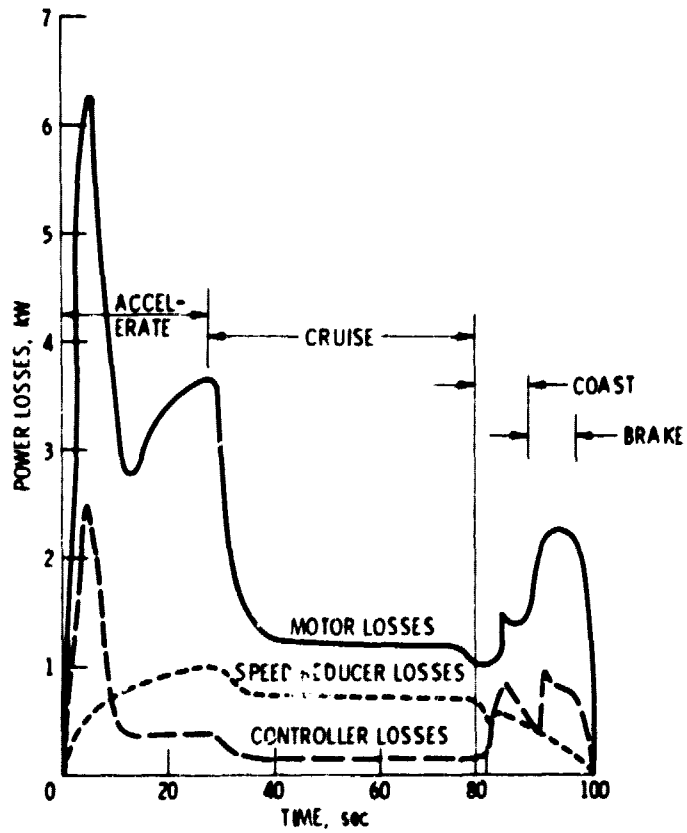


Figure 10. - Component power losses as a function of time for SAE J227a schedule "D" driving cycle.

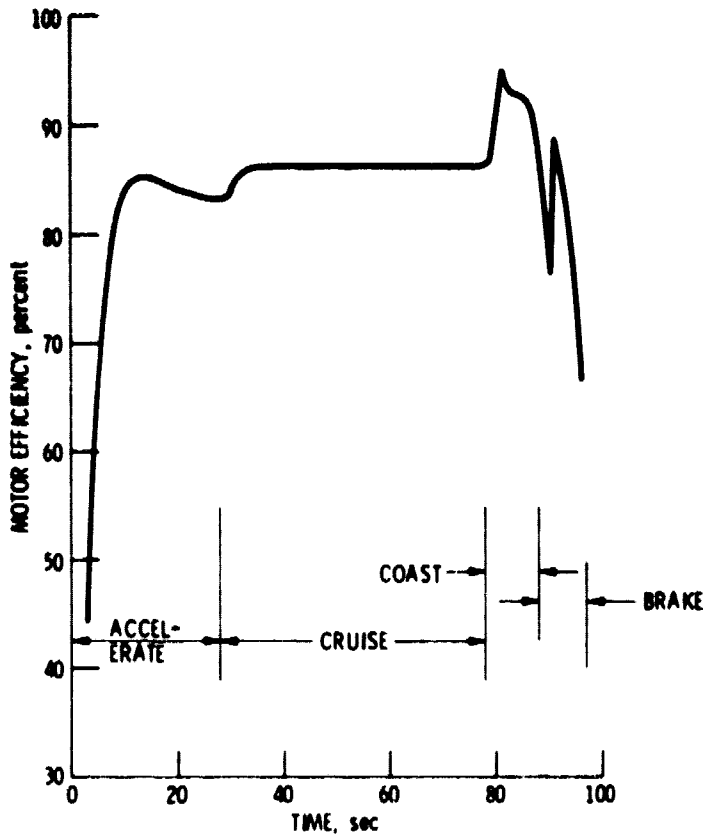


Figure 11. - Motor efficiency as a function of time for SAE J227a schedule "D" driving cycle.

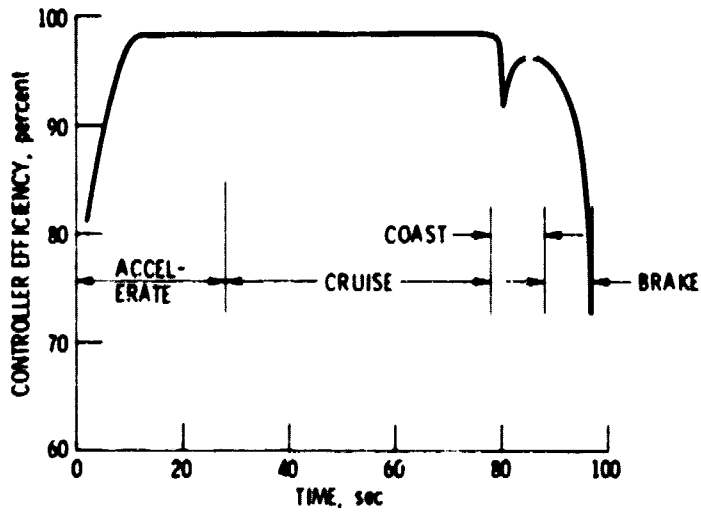


Figure 12. - Controller efficiency as a function of time for SAE J227a schedule "D" driving cycle.

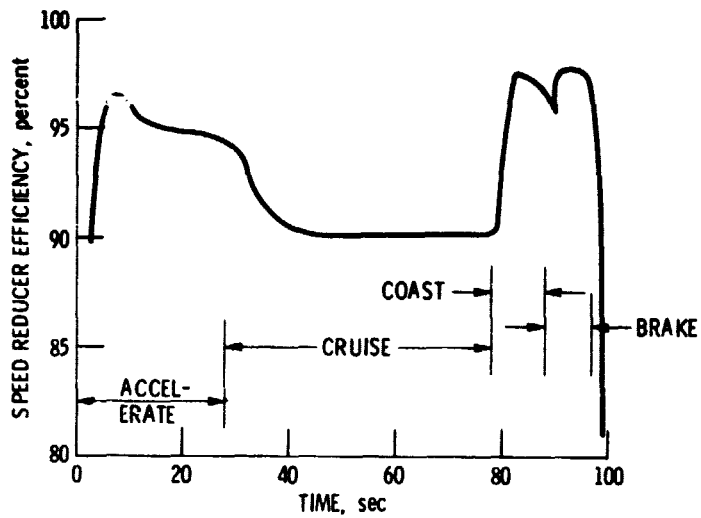


Figure 13. - Speed reducer efficiency as a function of time for SAE J227a schedule "D" driving cycle.

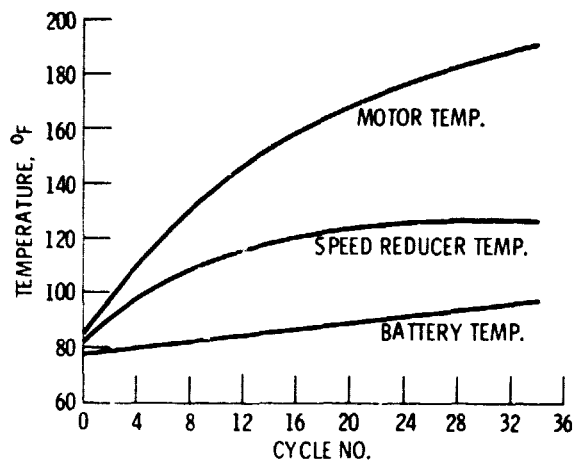


Figure 14. - Component temperature taken during "D" cycle range test.

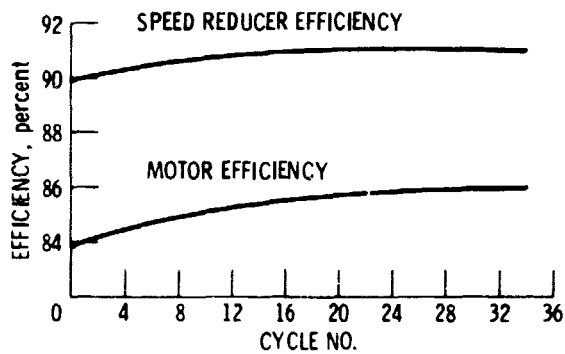


Figure 15. - Component efficiency taken during "D" cycle range test.